

Fully Quantitative Measurements of Differential Antibody Binding to Spike Proteins from Wuhan, Alpha, Beta, Gamma, Delta and Omicron BA.1 variants of SARS-CoV-2: Antibody Immunity Endotypes

Philip H. James-Pemberton¹, Shivali Kohli, Jordan Twynham, Aaron C. Westlake, Alex Antill, Jade Hunt, Rouslan V. Olkhov and Andrew M. Shaw^{1,2*}

¹Biosciences, University of Exeter, Stocker Road, Exeter, EX4 4QD, UK

²Attomarker Ltd, 3 Babbage Way, Exeter Science Park, Exeter, Devon, EX5 2FN, UK

Abstract

A fully quantitative comparative analysis of the differential binding to spike variant proteins to SARS-CoV-2 has been performed for the variants: Wuhan (ancestral strain), Alpha, Beta, Gamma, Delta and Omicron BA.1. Evolution of immunity through five patient cohorts was studied including pre-pandemic, first infection, first vaccine, second vaccine and triple-vaccinated cohorts. A series of immunity endotypes has been observed: U(+) showing protection to all variants; single, double, triple, quadruple and quintuple dropout endotypes U(±); some with no variant protection other than Wuhan vaccine spike U(-); and some unclassified, U(~). These endotypes may be imprinted. In the triple-vaccinated cohort ($n = 54$) there is a U(+) incidence of 65% (95% CI 51% - 76%) suggesting between half and three-quarters of the population have universal variant vaccine antibody protection; U(-) 6% (95% CI 2% - 15%) of the population have no variant antibody protection provided by the vaccine; and U(±) with at least one dropout has a incidence of 20% (95% CI 12% - 33%). Extending the cohort incidence to the population, up to 76% of the population may have an imprinted immunity endotype to an epitope that is effective against all variants; critical for both protection and binding to the ACE2 receptor: a universal immunity endotype. However, up to 33% of the population may have an immunity endotype that will never produce an effective antibody response to SARS-CoV-2 unless the immunity imprint is broken.

Funding – Exeter University Alumni, Attomarker Ltd funded PhD studentship at the University of Exeter and Attomarker Ltd funding directly.

Introduction

Vaccination has been adopted as the primary defence against SARS-CoV-2 and has brought the ongoing COVID-19 pandemic under significantly greater control. The initial mRNA vaccines were raised against the original Wuhan strain providing efficacy at both preventing infection and hospitalisation. The Pfizer vaccine had a reported efficacy of 93% for reducing symptomatic cases¹ 14 days or longer following the second dose. Similarly, for Astra Zeneca (AZ) with an equivalent efficacy of 69% – 74% in a real-world setting² and Moderna 95.2% efficacy (95% confidence limits 91.2 % – 97.4 %).³ As the SARS-CoV-2 variants have evolved, the vaccines have remained active at preventing hospitalisation but have differing efficacies at preventing infection and transmission, partly owing to waning immunity. Furthermore, the initial vaccination campaigns reached a high proportion of the population⁴ in some countries whilst take up for booster programmes has been more limited.

The key target of the vaccines has been the spike protein on the surface of the virus: only one vaccine has targeted the Nucleocapsid protein. Mutations of the spike for each of the major variants of concern, Alpha, Beta, Gamma, Delta and Omicron are shown in Figure 1 (Table S1) alongside the NIST standard human IgG presented on the same scale for comparison. The spike protein is 16.0 nm long and has a triangular, 3-fold symmetry cross-section,⁵ whereas IgG has dimensions of 14.5 nm × 8.5 nm × 4.0 nm.⁶ The S1 region of the S proteins is the most significantly mutated region principally around the receptor binding domain (RBD) binding to the ACE2 receptor and inducing changes to transmission and virulence of the infection. The description of antibody immunity is often restricted to the neutralising antibodies binding to RBD but the relative size and binding orientations point to a wider set of epitopes that would prevent receptor binding.

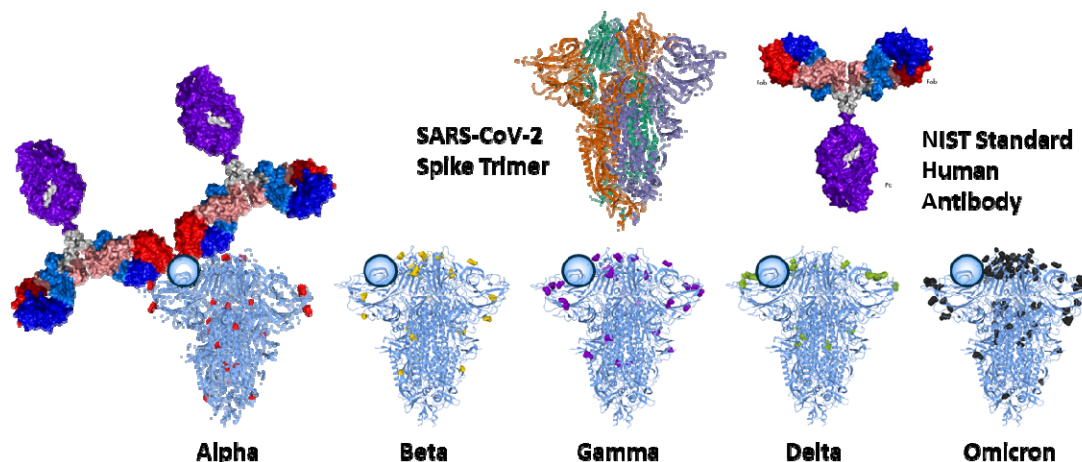


Figure 1 The spike protein for each of the variants of concern compared with the Wuhan version showing the different regions of mutation⁷. The structure of the NIST standard human antibody⁸ is included at the same scale. The circle is a 2 nm diameter region that does not contain mutations – a possible conserved binding site.

The host response to the vaccine and/or infection, raises several antibodies rapidly, which are then selected for those that provide immunity and subsequently “remembered” by memory B cells. Individual responses may vary across the spike protein leaving some individuals losing protection quickly if their selected epitopes are subject to mutation. Thus, individuals can potentially form immunological classes with different active epitopes which define mechanistically different responses to SARS-CoV-2 infection – antibody immunity

endotypes. Such endotypes differ from phenotypes because of the molecularly distinct mechanism of the response (as has been observed in asthma⁹) and support the role of immunity imprinting. Such underlying mechanisms will affect individual vaccine efficacy and may depend on previous or first infection.¹⁰ This could also explain why some individuals have frequent repeat infections.

Identification of the immunity endotypes requires a fully quantitative measure of antibody concentration that allows the differential binding between variant proteins to be analysed. Standardisation of immunoassay measures is possible for biophotonic sensor platforms with quantification based on the NIST standard human antibody.¹¹ In this paper, we investigate the antibody binding to the variant spike proteins for the Wuhan, Alpha, Beta, Gamma, Delta and Omicron BA.1 variants. The different variant proteins are screened with a panel of antibodies to establish epitope integrity for the calibration site in the S2 region and to map epitope degradation in the S1 region. Patient samples were screened from five cohorts: pre-pandemic (controls); the Wuhan wave pre-vaccine; and then single, fully vaccinated and boosted cohorts for select combinations of vaccines, boosters and infections. A classification of immunity endotype is derived from the observation of different immune responses.

Methods and Materials

Methods

Biophotonic Multiplexed Immuno-kinetic assay

A biophotonic platform, such as localised particle plasmon or continuous gold sensor, fundamentally consists of effective-mass sensors responding to the changes in refractive index in the plasmon field once it has been excited. The localised particle plasmon technique used here utilises an immuno-kinetic assay which has been described in detail elsewhere in a SARS-CoV-2 antibody sensing application.¹² Briefly, gold nanoparticles are printed into an array of 170 spots which are then individually functionalised with the SARS-CoV-2 spike proteins from each of the variants described in Table S1, alongside control spots of recombinant Human Serum Albumin for variation in illumination, temperature and non-specific binding. A protein A/G control channel measures total IgG and is used to assess antibody integrity in the calibration reagents.

The basic assay consists of a capture step, a detection step and a regeneration step with intervening wash steps. A video camera is used to monitor the brightness change in the scattered light from each of the spots on the array during this process. In the capture step, a diluted serum sample flows over the array. A wash step ensures non-specifically bound proteins are removed, including antibodies with low affinity. An IgG-specific detection step follows and the brightness change in the scattered light is integrated over 90s to form a quantitative measure of IgG binding. High and low controls are used to calibrate the sensor surface, repeated regularly to ensure quality control.¹³

The integrity of the protein samples on the surface was tested using a panel of antibodies raised to RBD, S1, S2 or whole S protein, detailed in Table S2. An anti-S2 antibody (40590-D001) was chosen for calibration as the corresponding epitope is present on all variants. The concentration of the antibody was calibrated against the NIST antibody RM8671, NISTmAb, a recombinant humanized IgG1k with a known sequence¹³ to assure monomeric purity of the antibody. High-control and low-control samples were made using the 40590-D001 antibody and these controls were then used to quantify results from human samples in units of mg/L.

Endotype classification was performed manually using a simple selection hierarchy algorithm leading to the definitions, Table 1. The classification is based on the instrument characteristics: Limit of Detection (LoD) = 0.2 mg/L and $10 \times \text{LoD}$ = limit of quantification (LoQ) = 2 mg/L. A full correlation analysis for all combinations of responses was also performed from which the correlation coefficients and lines of best fit were derived.

Table 1 Endotype classification and symbols used to represent them.

Endotype	Symbol	Classification
Universal Negative	U(-)	All antibody concentrations are $\leq \text{LoD}$ 0.2 mg/L
Universal Positive	U(+)	All antibody concentrations are > 2 mg/L (LoQ) and each concentration is $>10\%$ of the peak concentration (defined as the maximum concentration across all spike variants for that sample)
Dropout Endotypes	U(\pm)	
Single Dropout	<i>e.g.</i> W, α , β , γ , δ ,o (-)	A single antibody concentration is $<10\%$ of the peak concentration and that peak >2 mg/L
Double Dropout Subclasses	2(-) <i>e.g.</i> $\alpha\beta$ (-)	Two antibody concentrations are $<10\%$ of the peak concentration and that peak >2 mg/L (LoQ)
Triple Dropout Subclasses	3(-) <i>e.g.</i> $\alpha\beta\gamma$ (-)	Three antibody concentrations are $<10\%$ of the peak concentration and that peak >2 mg/L (LoQ)
Quadruple Dropout Subclasses	4(-) <i>e.g.</i> $\alpha\beta\gamma\delta$ (-)	Four antibody concentrations are $<10\%$ of the peak concentration and that peak >2 mg/L (LoQ)
Quintuple Dropout Subclasses	5(-) <i>e.g.</i> $\alpha\beta\gamma\delta\text{o}$ (-)	Five antibody concentrations are $<10\%$ of the peak concentration and that peak >2 mg/L (LoQ)
Unclassified	U(~)	All results are ≥ 0.2 mg/L (LoD), but not all >2 mg/L (LoQ). No large disparities in concentration between variants.

The incidence in each of the endotype groups is calculated as a simple percentage proportion with Wilson 95% confidence limit estimates.

Materials

Materials used throughout the course of the experiments were used as supplied by the manufacturer, without further purification. Sigma-Aldrich supplied phosphate buffered saline (PBS) in tablet form (Sigma, P4417), phosphoric acid solution (85 ± 1 wt. % in water, Sigma, 345245) and Tween 20 (Sigma, P1379). Glycine (analytical grade, G/0800/48) was provided by Fisher Scientific. Assay running and dilution buffer was PBS with 0.005 v/v % Tween 20 and the regeneration buffer was 0.1 M phosphoric acid with 0.02 M glycine solution in deionized water.

The recombinant human antibody to the spike protein S2 subdomain was a chimeric monoclonal antibody (SinoBiological, 40590-D001, Lot HA14AP2901). The antibody was raised against recombinant SARS-CoV-2 / 2019-nCoV Spike S2 ECD protein

(SinoBiological, 40590-V08B). The panel of antibodies seen in Table S2 were used to screen antigens for relative integrity and epitope presentation.

NISTmAb, a recombinant humanized IgG1 κ with a known sequence¹³ specific to the respiratory syncytial virus protein F (RSVF)¹⁴, was from National Institute of Standards and Technology (RM8671). The detection mixture consisted of a 200-fold dilution of IG8044 R2 from Randox in assay running buffer. The sensor chips were printed with recombinant human serum albumin from Sigma-Aldrich (A9731), protein A/G from ThermoFisher (21186), and six SARS-CoV-2 Spike Protein variants for the Wuhan, Alpha, Beta, Delta, Gamma and Omicron strains from SinoBiological as detailed in Table S3.

Patient Samples

Commercial samples

Serum samples was purchased from two suppliers (Biomex GmbH and AbBaltis). 17 pre-pandemic (pre-December 2019), PCR(-) human serum samples were purchased from AbBaltis. All were tested and found negative for STS, HbsAg, HIV1 Ag (or HIV PCR(NAT)), HIV1/2 antibody, HCV antibody and HCV PCR(NAT) by FDA approved tests. 11 positive samples were purchased from AbBaltis which were all from PCR(+) individuals. No information was provided regarding symptoms of the donors. 45% of these samples were from female donors and 55% were from male donors. The age of donors ranged from 19 to 81 years. No information on time from infection to sample collection was given.

Samples purchased from Biomex ($n=26$) were from PCR(+) individuals. All samples were YHLO Biotech SARS-CoV-2 IgG positive and Abbott SARS-CoV-2 IgG positive. A spectrum of patient symptoms from the following list were detailed for each sample: fever, limb pain, muscle pain, headache, shivers, catarrh, anosmia, ache when swallowing, diarrhoea, breathing difficulties, coughing, tiredness, sinusitis, pneumonia, sickness, lymph node swelling, pressure on chest, flu-like symptoms, blood circulation problems, sweating, dizziness, and hospitalisation. Time from infection to sample collection ranged from 27 to 91 days. 35% of these samples were from female donors and 65% were from male donors. The samples were collected prior to June 2020, so PCR(+) samples will result from infection by the SARS-CoV-2 strains circulating prior to this time, most similar to the Wuhan protein. These commercial samples, 38(+) and 16(-), were tested using the Spike Variant Array as a part of this study.

Attomarker Clinic samples

Samples were collected from patients in Attomarker clinics, all of whom provided informed consent for their anonymised data to be used in research to aid the pandemic response. The data from tests of 101 patient samples are included in this study: 16 had received one dose of either AZ, Pfizer or Moderna SARS-CoV-2 vaccine; 40 had received two doses of either AZ, Pfizer or Moderna SARS-CoV-2 vaccine at least 14 days prior to sample collection and testing by Attomarker; 43 further samples were from patients who had received a third vaccination. Full patient demographics are shown in Table S3.

Ethical Approval

The use of the Attomarker clinical samples was approved by the Bioscience Research Ethics Committee, University of Exeter.

Results

A chimeric monoclonal antibody to the S2 region of the Spike protein was used to assess protein integrity on the surface and calibrate the relative binding capacity of each channel. The maximum binding signal (θ_{\max}) values were determined by fitting to a Langmuir Adsorption model and are presented in Table S4. The binding for all samples to the different variant spike proteins is shown in Figure 2 and the medians and quartiles are shown in Table S5.

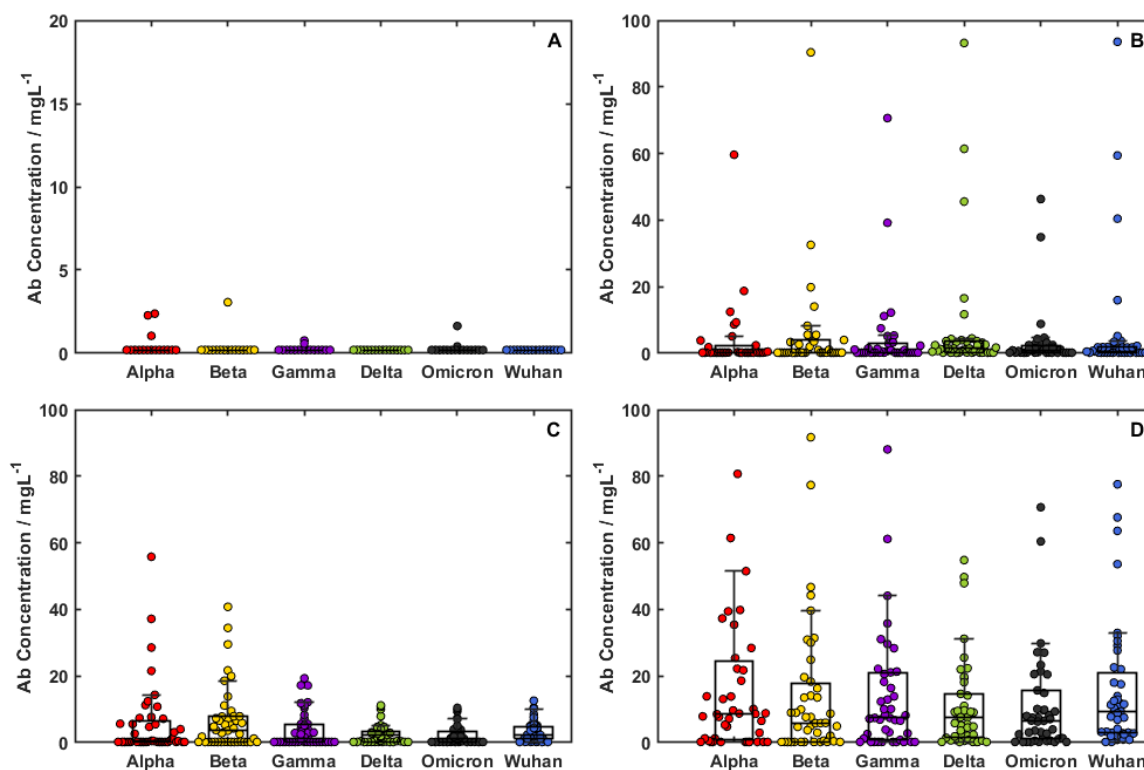


Figure 2. The antibody distributions in four patient cohorts: A) pre-pandemic samples, B) Wuhan (+) samples from May 2020, C) Double-vaccinated samples (AZ or Pf), D) Triple-vaccinated samples

The population analysis of spike protein binding does not show the individual, personalised sample variations that allow endotype classification based on the definition and hierarchy in Table 1, some examples of which are shown in Figure 3. The universal response endotype, U(+), shows a good antibody response to all variants (Figure 3A); the ideal vaccine candidate, whereas the universal negative, U(-), (Figure 3B) shows no responses above the LoD (0.2 mg/L) in the bioassay used herein. The unclassified samples, U(-), (Figure 3C) amounts to 25% of the entire sample set and is controlled by the LoD parameter: no correction for antibody waning has been made to allow for the period between vaccination and test. The more interesting profiles are those with variant dropout such as $\beta(-)$ (Figure 3D), $\alpha(-)$ (Figure 3E), and the profiles showing $W\alpha(-)$, $\alpha\beta\gamma(-)$ and $W\alpha\gamma\delta(-)$ but response to some other variant proteins, in Figure 3F, G, and H. Some samples showed only a single variant response as in Figure 3I, which exhibits a $W\alpha\gamma\delta\alpha(-)$ pattern of variant dropout.

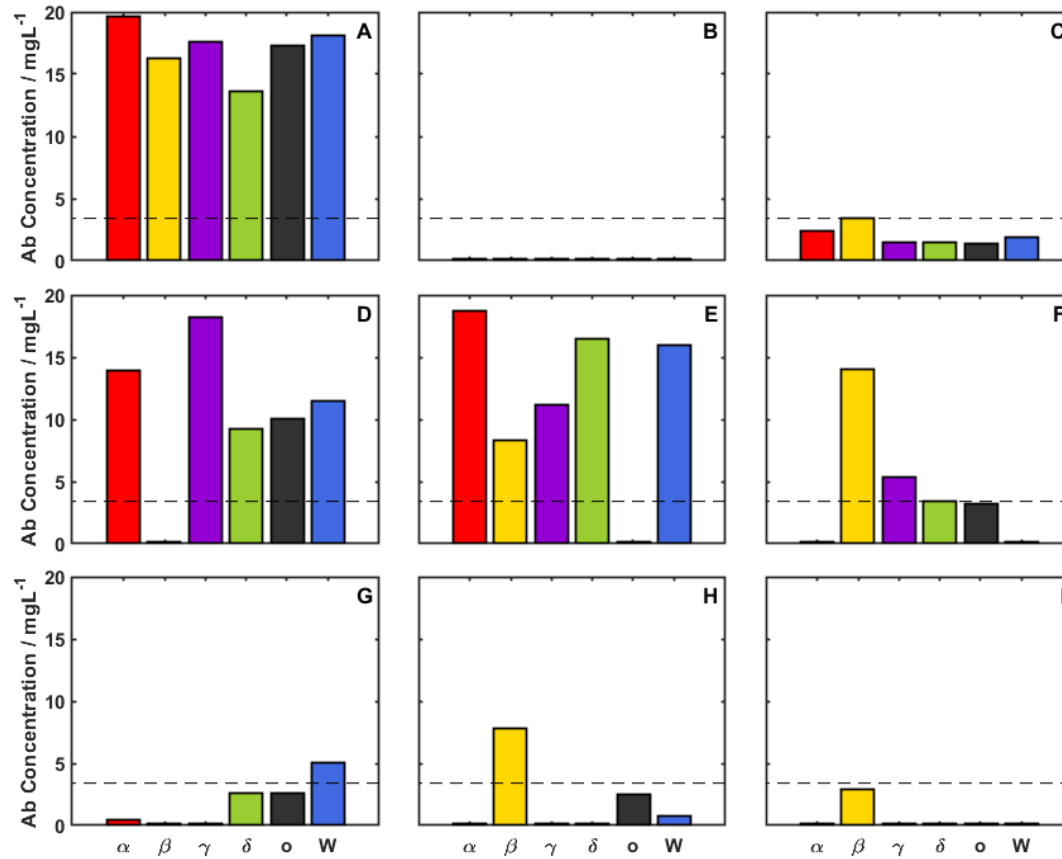


Figure 3. The endotypes identified in this study: A) Universal Positive (2xAZ), B) Universal Negative (3xPf), C) Unclassified (W(+)), D) $\beta(-)$ dropout (3xVacc), E) $o(-)$ dropout (W(+)), F) $W\alpha(-)$ dropout (W(+)), G) $\alpha\beta\gamma(-)$ dropout(2xAZ), H) $\alpha\gamma\delta W(-)$ dropout (2xAZ), I) $W\alpha\gamma\delta o(-)$ dropout (1xAZ). The dotted threshold is set at 3.4 mg/L, the mucosal recovery thresholds derived elsewhere.¹⁵

The incidences of each endotype in the patient cohorts is detailed in

Table 2 with the cohort summary showing U(-) dominating the pre-pandemic cohort, 25% U(~), but 19% showing dropouts in W(-) indicating pre-pandemic antibodies with paratopes to different epitopes on the variant spike proteins. The incidence of U(+) increases through the vaccination cohorts reaching 50% - 100% in the triple vaccinated. Detailed endotype analysis shows there are some dropouts amongst the vaccine cohorts, notably β (-) for those with Pf vaccination histories.

Results of the correlation analysis (Table S6) and the least-squares gradients (Table S7) show good correlation between the variant concentrations in the early pandemic (pre-vaccination) cohort, W(+), deriving immunity from natural infection only. The correlation shows some conspicuously poor coefficients in the vaccination cohort involving the β and all other spike variant proteins, again associated with a Pf vaccination history.

Table 2 Incidences of each of the endotype classifications, for each of the patient cohorts. One patient with No Vaccination and a U(+) endotype has been omitted from the table. (UN is undeclared)

Endotype	Overall Incidence (%)	Pre-Pan (16)	W(+) (38)	Endotype Incidence (%) by Cohort												Und	
				1x Vaccine		2x Vaccine			3x Vaccine								
				AZ (8)	Pf (3)	AZ (26)	Pf (17)	UN (1)	AZ- (14)	AZ- (9)	Pf- (11)	Pf- (3)	Nx- (1)	M- (1)	UN (5)		UN (1)
Summary																	
U(+)	31.2		18.4	25.0		30.8	17.6		57.1	100	45.5	33.3		100	60.0		100
U(-)	13.0	56.3	10.5	25.0	33.3	7.7			7.1		9.1						
U(~)	26.0	25.0	31.6			34.6	47.1	100	14.3		27.3						
U(±) Any	29.9	18.8	39.5	12.5	0.0	26.9	35.3		21.4		18.2	66.7	100		40.0		
Dropout Endotypes U(±)																	
Single																	
α(-)	3.9		5.3	25.0		3.8			7.1								
β(-)	1.9								7.1		9.1				20.0		
γ(-)	0.6						5.9										
δ(-)	0.0																
α(-)	1.3		5.3														
W(-)	1.3		5.3														
Total	9.1		15.8	25.0		3.8	5.9		14.3		9.1				20.0		
Double (-)																	
βγ(-)	0.6		2.6														
βo	0.6		2.6														
αW	1.3		5.3														
δW	0.6					33.3											
αγ	0.6						5.9										
αδ	0.6						5.9										
Total	4.5		10.5			33.3											
Triple (-)																	
αδW	0.6		2.6														
αβγ	3.9							7.7	11.8			66.7					
αγδ	0.6					33.3							100				
αγo	1.3														20.0		
βγo	0.0																
Total	6.5		2.6			33.3		7.7	11.8			66.7	100		20.0		
Quadruple(-)																	
αγδW	1.9	6.3						7.7									
αβγW	1.3		5.3					3.8									
αβδW	1.3		2.6					3.8									
αδoW	0.6																
αβγo	1.9								5.9		7.1		9.1				
Total	7.1	6.3	7.9					15.4	5.9		7.1		9.1				
Quintuple (-)																	
βγδoW	1.3	12.5															
αβγoW	0.6		2.6														
αγδoW	0.6			12.5													
Total	2.6	12.5	2.6	12.5													

Discussion

The effectiveness of a vaccine program to SARS-CoV-2 changes as different variants arise. If society is to live with and better manage the virus then an effective, pan-variant vaccine would be ideal. However, the high global virus prevalence is allowing production of new variants, with significant mutations occurring every 70 days in the case of Omicron subvariants.¹⁶ Different variants can lead to vaccine evasion and escape, and development of a new targeted vaccine takes at least 100 days,¹⁷ by which time further mutations may have occurred. Not only is vaccine efficacy vulnerable to mutation, serology tests and immunotherapy are also optimised against specific variants: all of which will need updating on the same pandemic timescale. These pandemic timescales need to change to allow the successful transition from pandemic to endemic, requiring the next generation vaccines, therapies, tests and containment measures to have extended utility periods.

Essential to optimising vaccines is understanding how structure-function of the antibodies is altered with mutations of the spike protein, Figure 1. The mRNA vaccines produce the entire spike protein in isolation which allows the host immune response to be tailored to the S1 and S2 regions of the protein. In an infection, the immunological less relevant S2 region would be obscured by the viral envelope. A wider hemispherical region at the top of the spike S1 region, Figure 1, is relevant to antibody protection¹⁸ both neutralisation and opsonisation not restricted to RBD-binding antibodies. Effective neutralising epitopes approximately 2 nm in diameter can be present within this hemisphere still prevent ACE2 binding. The host response is optimised to all protective epitopes, producing memory B cells and T cells with chosen epitope regions of the proteins, potentially unique to each host and leading to immunity imprinting.¹⁹⁻²¹

This study has looked at the host response from patient cohorts with early pandemic infection, and single, double, and boosted vaccination histories. The host response to the Wuhan, ancestral spike protein and Alpha, Beta, Gamma, Delta, and Omicron BA.1 variants were also measured. No single reference material exists (WHO international standard material²²) to allow comparison directly between these variants. The existence of U(+) endotype suggests a conserved epitope (or epitopes) on the S2 part of the protein and a panel of antibodies have been used to characterise this epitope integrity, Table S2. The chosen reference antibody, (SinoBiological 40590-D001) was calibrated against the NIST standard antibody to convert all assay results to mg/L.

The distributions of the data in Figure 2 (Table S5) show improved median responses with vaccination in the boosted cohort. The Wuhan spike protein, the target of the vaccines, produces the largest median response with smaller responses to the variants. The interquartile ranges vary however, from 3 to 17 mg/L for the Wuhan variant vaccine response. There is a significant spectrum of immunity in the population, some of which may not be protective against infection even after the booster vaccination, and remains subject to waning at differential rates (reported to range between 60 and 200 days, with a mean of 106 days²³). A protection threshold against infection has been sought and there are some candidate levels¹⁵ which would suggest a personalised smart boosting strategy, potentially with different vaccine choices.

It is of note however, that the population distributions mask individual antibody immunity responses, which show 7 endotypes and one unclassified class, Figure 3. The immunity endotypes discovered here-in are based on the mechanistic binding to variant spike proteins conferring protection, at concentrations in the mucosa derived from both vaccination and

recovery responses.^{15,24} The ideal endotype is the universal positive endotype, U(+), which has antibodies binding to all variants. The other extreme is the universal negative, U(-) which has no antibody binding. The incidence of U(+) in the triple-vaccinated cohort varies from 43% to 100% depending on the vaccination history and U(-) 0% – 7%. There is an incidence of 14% – 23% of variant dropout of one of the multiple types. Treating the triple-vaccinated cohorts as one (heterogeneously derived from a mixture of infection and triple-vaccination histories, $n = 54$), gives a U(+) incidence of 65% (95% CI 51% - 76%) suggesting between half and three-quarters of the population have universal variant vaccine protection; U(-) occurs in 6% (95% CI 2% - 15%) of the tests suggesting that the corresponding population has no protection from the vaccine; and U(\pm) with at least one dropout has a prevalence of 20% (95% CI 12% - 33%). Speculatively, those patients who are vaccine-hesitant will likely have a mixture of natural immunity from the different variants, depending on the prevalent variant at the time of infection.

Detailed analysis of the different dropout endotypes show that single, triple and quadruple dropouts dominate the triple-vaccinated cohort; 17% (95% CI 9%-29%) contain the β dropout as one of the endotype components, as supported by the significantly lower correlation coefficients involving β and other components. The β -dropout endotype appears to be associated strongly with the Pfizer vaccine anywhere in the vaccination-infections history. Most W-dropout endotypes are pre-pandemic which accounts for all quintuple dropouts and suggests potential circulating coronavirus-induced immunity, seemingly from homogenous regions of the spike protein between the two subtypes.²⁵ Interestingly, the $\delta W(-)$ samples in the AZ single vaccinated cohort all had β -led responses suggesting exposure to the β variant and consequent imprinting, and thus worthy of larger cohort exploration.

The formation of vaccine-infection endotypes and the process of immune imprinting has been previously suggested,^{26,27} and has been reported following repeated exposure to different circulating strains of influenza,²⁸ with the first exposure potentially setting the imprint.²⁹ Therefore, these immunity endotypes may form part of the same immunity imprinting concept; repeated challenges of any variant or vaccine will re-start synthesis of the same antibody endotype already present and optimised from previous exposures. These considerations provide a potential explanation to previous observations of potent cross-reactive antibody production following exposure to Omicron, despite less well-optimised antibody production to Omicron itself.¹⁰ The correlation coefficients analysed here-in implicate a need to screen variant proteins, particularly Wuhan and β , in order to assess immunity endotype imprinting.

The next challenge is to either break the imprint or tolerate up to 33% of the population having a limited or no response to future SARS-CoV-2 variants. These immunity endotypes may be particularly vulnerable to repeat infections. The emergence of further mutated epitopes can also increase the risk of a decreased overall paratype affinity, suggesting higher levels of circulating antibodies required to prevent re-infection. The vaccine attachment kinetics and affinity molecular mechanism result in the manifestations of vaccine escape may explain why two- or three-doses of vaccination are protective against severe disease and hospitalization but have poorer protection against transmission.³⁰⁻³²

Conclusions

Antibody immunity screening with various patient cohorts at different stages of vaccination points to immunity endotypes which may be imprinted following first exposure. Up to 76% of the population may have good universal protection against all the tested variants here and may have antibodies to epitopes in critically conserved regions of the spike protein, such as those necessary for ACE2 receptor binding or associated conformational changes. The structure-function analysis and mutation analysis point towards mutation-free regions, Figure 4, not in the receptor binding domain but in the hinge region that allows the conformational change from pre-fusion to fusion configurations. These regions are difficult to mutate without losing function and so represent regions conserved, Achilles' heel, epitopes. These are ideal vaccine targets.

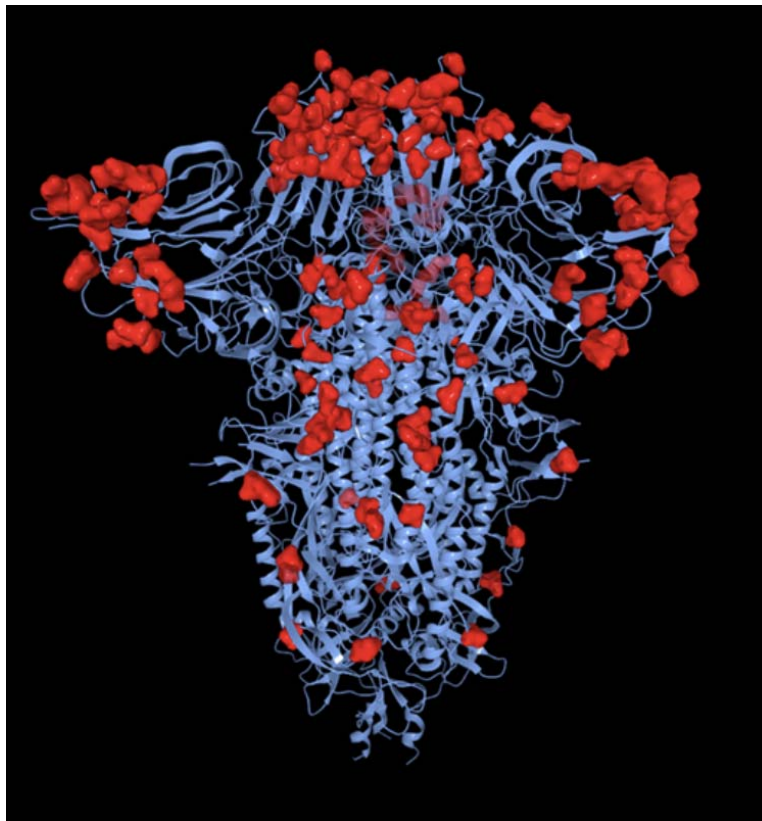


Figure 4 The Wuhan Spike protein structure showing all mutations for Alpha, Beta, Gamma and Delta variants.

That leaves up to 16% of the population with no protection and up to 33% of the population with limited protection, alongside an imprinted endotype that may never make protective antibodies. These dropout endotypes now form new at-risk groups for vaccination which are not captured by age alone. Breaking the imprint may be possible with alternative presentations of the target protein such as in the whole neutralized viral particles or protein vaccines. Better still, a more structurally relevant presentation of epitopes may trigger different antigen-presenting-cell signals and thus lead to a re-optimisation of antibody production.³³ These mechanistic intervention targets could be derived from quantitative structure-function analyses and are important in preventing vaccine escape.

Acknowledgements

The authors would like to thank Dr Jonathan Snicker for their guidance on the potential strategic and policy implications of the scientific findings.

References

1. Dagan N, Barda N, Kepten E, et al. BNT162b2 mRNA Covid-19 Vaccine in a Nationwide Mass Vaccination Setting. *New England Journal of Medicine* 2021; **384**(15): 1412-23.
2. Mallapaty S, Callaway E. What Scientists do and don't know about the Oxford-AstraZeneca COVID vaccine. *Nature* 2021; **592**: 15-7.
3. Baden LR, El Sahly HM, Essink B, et al. Efficacy and Safety of the mRNA-1273 SARS-CoV-2 Vaccine. *The New England journal of medicine* 2021; **384**(5): 403-16.
4. Lazarus JV, Ratzan SC, Palayew A, et al. A global survey of potential acceptance of a COVID-19 vaccine. *Nat Med* 2021; **27**(2): 225-8.
5. Walls AC, Park Y-J, Tortorici MA, Wall A, McGuire AT, Veesler D. Structure, Function, and Antigenicity of the SARS-CoV-2 Spike Glycoprotein. *Cell* 2020; **181**(2): 281-92.e6.
6. Tan YH, Liu M, Nolting B, Go JG, Gervay-Hague J, Liu G-y. A nanoengineering approach for investigation and regulation of protein immobilization. *ACS Nano* 2008; **2**(11): 2374-84.
7. ViralZone SSIoB. Spike Protein Figure. 2022. <https://viralzone.expasy.org/9556> (accessed 21 June 2022).
8. NIST. <https://www.nist.gov/image/nistmabmonoclonalantibodyjpg>; 2015.
9. Kuruvilla ME, Lee FE, Lee GB. Understanding Asthma Phenotypes, Endotypes, and Mechanisms of Disease. *Clin Rev Allergy Immunol* 2019; **56**(2): 219-33.
10. Reynolds CJ, Pade C, Gibbons JM, et al. Immune boosting by B.1.1.529 (Omicron) depends on previous SARS-CoV-2 exposure. *Science* 2022: eabq1841.
11. Schiel JE, Turner A, Mouchahoir T, et al. The NISTmAb Reference Material 8671 value assignment, homogeneity, and stability. *Analytical and bioanalytical chemistry* 2018; **410**(8): 2127-39.
12. Shaw AM, Hyde C, Merrick B, et al. Real-world evaluation of a novel technology for quantitative simultaneous antibody detection against multiple SARS-CoV-2 antigens in a cohort of patients presenting with COVID-19 syndrome. *Analyst* 2020.
13. Formolo T LM, Levy M, Kilpatrick L, Lute S, Phinney K, et al. . Determination of the NISTmAb primary structure. State-of-the-Art and Emerging Technologies for Therapeutic Monoclonal Antibody Characterization: ACS Symposium Series; 2015: 1-62.
14. McLellan JS, Chen M, Kim A, Yang Y, Graham BS, Kwong PD. Structural basis of respiratory syncytial virus neutralization by motavizumab. *Nature structural & molecular biology* 2010; **17**(2): 248-50.
15. James-Pemberton PH, Helliwell MW, Olkhov RV, et al. Fully Quantitative Measurements of the Antibody Levels for SARS-CoV-2 Infections and Vaccinations calibrated against the NISTmAb Standard IgG Antibody. *medRxiv* 2022: 2022.07.12.22277533.
16. Institute S. 2022. <https://covid19.sanger.ac.uk/lineages/raw> (accessed September 2022).
17. Pfizer. Pfizer and BioNTech Provide Update on Omicron Variant. 2021.
18. Harvey WT, Carabelli AM, Jackson B, et al. SARS-CoV-2 variants, spike mutations and immune escape. *Nature Reviews Microbiology* 2021; **19**(7): 409-24.
19. Röltgen K, Nielsen SCA, Silva O, et al. Immune imprinting, breadth of variant recognition, and germinal center response in human SARS-CoV-2 infection and vaccination. *Cell* 2022; **185**(6): 1025-40.e14.
20. Wheatley AK, Fox A, Tan HX, et al. Immune imprinting and SARS-CoV-2 vaccine design. *Trends Immunol* 2021; **42**(11): 956-9.
21. Reynolds CJ, Pade C, Gibbons JM, et al. Immune boosting by B.1.1.529 (Omicron) depends on previous SARS-CoV-2 exposure. *Science* 2022; **377**(6603): eabq1841.
22. Kristiansen PA, Page M, Bernasconi V, et al. WHO International Standard for anti-SARS-CoV-2 immunoglobulin. *Lancet* 2021; **397**(10282): 1347-8.
23. Dan JM, Mateus J, Kato Y, et al. Immunological memory to SARS-CoV-2 assessed for up to 8 months after infection. *Science* 2021; **371**(6529): eabf4063.
24. James-Pemberton PH, Helliwell MW, Olkhov RV, et al. Vaccine, Booster and Natural Antibody Binding to SARS-CoV-2 Omicron (BA.1) Spike Protein and Vaccine Efficacy. *medRxiv* 2022: 2022.07.12.22277539.
25. Cueno ME, Imai K. Structural Comparison of the SARS CoV 2 Spike Protein Relative to Other Human-Infecting Coronaviruses. *Frontiers in Medicine* 2021; **7**.
26. Reynolds Catherine J, Pade C, Gibbons Joseph M, et al. Immune boosting by B.1.1.529 (Omicron) depends on previous SARS-CoV-2 exposure. *Science*; **0**(0): eabq1841.
27. Reynolds Catherine J, Gibbons Joseph M, Pade C, et al. Heterologous infection and vaccination shapes immunity against SARS-CoV-2 variants. *Science* 2022; **375**(6577): 183-92.
28. Yang B, Lessler J, Zhu H, et al. Life course exposures continually shape antibody profiles and risk of seroconversion to influenza. *PLOS Pathogens* 2020; **16**(7): e1008635.
29. Zhang A, Stacey HD, Mullarkey CE, Miller MS. Original Antigenic Sin: How First Exposure Shapes Lifelong Anti-Influenza Virus Immune Responses. *The Journal of Immunology* 2019; **202**(2): 335.

30. Collie S, Champion J, Moultrie H, Bekker L-G, Gray G. Effectiveness of BNT162b2 Vaccine against Omicron Variant in South Africa. *New England Journal of Medicine* 2021; **386**(5): 494-6.
31. Tseng HF, Ackerson BK, Luo Y, et al. Effectiveness of mRNA-1273 against SARS-CoV-2 Omicron and Delta variants. *Nature Medicine* 2022; **28**(5): 1063-71.
32. Andrews N, Stowe J, Kirsebom F, et al. Covid-19 Vaccine Effectiveness against the Omicron (B.1.1.529) Variant. *New England Journal of Medicine* 2022; **386**(16): 1532-46.
33. Valneva. Vaccine Candidate VLA2001. 2021.